Dynamical chaos in a minimum system of truncated Euler equations

Eugene Levich
Benjamin Levich Center for Turbulence Research, Division of Ormat Industries Ltd., P.O. Box 68, Yavneh 70650, Israel

Boris A. Malomed*
Department of Interdisciplinary Studies, Faculty of Engineering, Tel Aviv University, Tel Aviv 69978, Israel

Rossella Monti
Department of Civil Engineering, Brescia University, via Branze 38, 25123 Brescia, Italy

Leonid Shtilman and David Tsibelman
Department of Fluid Dynamics and Heat Transfer, Faculty of Engineering, Tel Aviv University, Tel Aviv 69978, Israel
(Received 27 February 1997; revised manuscript received 29 May 1997)

We derive a finite-dimensional Hamiltonian dynamical system, projecting the Euler equations onto a basis composed of six wave vectors closed into a tetrahedron with equal edges. We obtain a system of twelve equations for complex amplitudes of the flow, with three integrals of motion (IM's), namely, the energy (E), helicity (H), and an additional one related to the squared angular momentum. The system admits reduction to six complex equations and finally to six real ones for three positive-helicity and three negative-helicity modes, which is the *minimum* dynamical system to approximate the three-dimensional Euler equations. We simulate the latter system numerically and demonstrate that it is partly chaotic despite having the same three IM's in its six-dimensional phase space. The simulations reveal that the dynamics is fully chaotic in some region of the phase space, while in another region it is mixed: at the same set of values of IM's, some trajectories are chaotic and some are regular. A chart showing the fully chaotic and mixed regions is obtained, in the first approximation, in the space of the IM's values. To quantify the chaos, we compute the mean Lyapunov exponent (LE) Λ characterizing the local instability of the trajectories. We find that Λ is nearly independent of the choice of the trajectory at fixed values of IM's in the fully chaotic region, i.e., this region appears to be ergodic. Generally, the system is ''most chaotic'' at zero helicity and it is apt to become ''less chaotic'' with an increase of H/E. We demonstrate, in accord with this, that Λ is a monotonically decreasing function of H/E in the chaotic region, but inside the region of the mixed behavior the dependence is not monotonic. We also report some results obtained for a more general system of six complex equations. A preliminary inference is that there is no drastic qualitative difference from the system of six real equations, though a change (*decrease*) of LE can be conspicuous. A simple dissipative generalization of the model is considered too. [S1063-651X(97)04409-7]

PACS number(s): 05.45.+b, 47.27.Eq

I. INTRODUCTION

Attempts to approximate turbulent flows by finite-dimensional dynamical systems (DS's) are aimed at understanding gross features of turbulence in terms of simple models [1]. In particular, a DS based on the statistical Karhunen-Loeve eigenfunction decomposition with subsequent selection of just three important modes provides a remarkable model of wall-bounded turbulent flows [2]. A model of another kind was put forth in [3]. It was based on an expansion of the Euler equations over eigenflows of the curl operator with positive and negative helicities. The quadratic nonlinearity in the Euler equations naturally gives rise to triplet interactions of different types between the modes. It was demonstrated that the interactions that involve modes with helicities of the same sign give rise only to an inverse cascade, while the interactions mixing modes with different signs of the helicity transfer the energy down to small scales.

However, the decomposition based on the curl eigenflows was not used in [3] for the derivation of an actual DS to model the turbulence. Steps in this direction will be made in the present work. In order to construct a nontrivial model, we will consider the simplex in the three-dimensional (3D) space formed by the corresponding wave vectors, viz., a regular tetrahedron. Projecting the full Euler equations onto this basis, in Sec. II we derive a DS for 12 complex amplitudes of the flow. The system has three integrals of motion (IM's), two of them exactly corresponding to the energy (E) and helicity (H) of the 3D Euler equations, while the meaning of the third IM, to be designated I, is less clear, although it may be related to the squared angular momentum of the moving fluid. We notice that the system admits a reduction to an invariant subsystem for six complex variables, which assumes that each edge of the underlying tetrahedron is carrying either positive or negative helicity. Thus we have three positive-helicity and three negative-helicity modes.

In the structure of the latter system, one can easily distinguish two coupled subsystems, each containing three equa-

*Electronic address: malomed@eng.tau.ac.il

tions. The subsystems can be readily cast into an explicitly Hamiltonian form (i.e., the corresponding simplectic structures can be defined), so that each conserves its own Hamiltonian. These two Hamiltonians are linear combinations of E and H.

A symmetry of the DS for the six complex amplitudes admits a further invariant reduction to six *real* variables. After both reductions, the system keeps the same three IM's. This finally reduced DS appears to be a *minimum* truncated model of the 3D Euler equations and it is the main subject of the present work. It is relevant to stress that, according to the Liouville theorem, a Hamiltonian six-dimensional DS is completely integrable in the presence of three IM's, provided that the system's phase space is endowed with a usual simplectic structure (i.e., one can identify it as a system with three degrees of freedom). A reason for our system to remain chaotic is its noncanonical simplectic structure.

Results of numerical simulations are presented in Sec. III. We find that, in certain regions of values of the three IM's, all the dynamical trajectories are definitely chaotic. To quantify the chaos, we compute the mean Lyapunov exponent (LE) Λ characterizing the local instability of a given trajectory [5]. We find that, in these completely chaotic regions, Λ is almost independent of the choice of a particular trajectory at fixed values of IM's. In other words, the system appears to be ergodic in the chaotic regions. In some other regions, both chaotic and regular trajectories are generated by different initial conditions having equal values of the IM's. Obviously, in these mixed regions the system is not ergodic, although Λ can be defined in this case too for those trajectories that are chaotic. We have not found any region where *all* the trajectories would be regular.

We delineate a boundary between the purely chaotic and mixed regions in the parametric plane $(H/E, I/E)$. Generally, the system is ''most chaotic'' at zero helicity and is apt to become ''less chaotic'' with an increase of H/E (in the limit $H/E \to 1$, the dynamics becomes trivial). To describe the chaotic properties of the model more accurately, we plot Λ vs H/E at different fixed values of I/E, which allows us to scan the above-mentioned parametric plane along a system of parallel cuts (we also add some perpendicular cuts). An inference is that the dependence $\Lambda(H/E)$ is monotonically decreasing if the cut does not cleave the region of the mixed behavior. In the opposite case, the dependence $\Lambda(H/E)$ demonstrates several oscillations.

In Sec. IV we briefly consider the above-mentioned more general DS consisting of six complex equations, a reduction of which leads to the real system studied in detail in Sec. III. We take a few typical chaotic and regular dynamical trajectories of the real system and consider perturbed trajectories of the complex system, obtained by adding small imaginary parts to the initial values of the dynamical variables. We conclude that, most typically, the regular and chaotic trajectories remain, respectively, regular and chaotic after adding a small complex perturbation, though the LE of the perturbed chaotic trajectory may become essentially *smaller*. In Sec. V we consider a modified version of our DS including losses and gain. The result is that the dynamics of the dissipatively perturbed model is asymptotically equivalent to that of the conservative one at specially selected values of E and H. Concluding remarks are collected in Sec. VI.

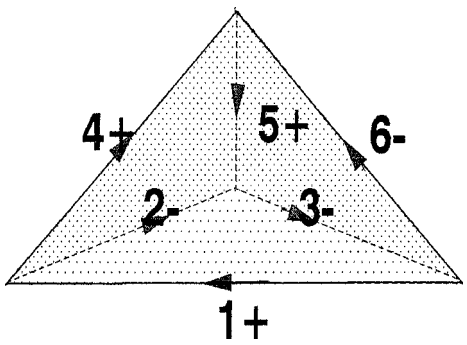

FIG. 1. Six wave vectors that are the basis of the truncated dynamical system. The digits on each edge indicate the numbers of the corresponding amplitude, while the signs show which particular helicity is chosen for the edge.

II. DERIVATION OF THE SYSTEM

The helical eigenmodes of the 3D velocity field $\mathbf{v}(\mathbf{r})$ are determined as solutions to the equation [4] $\nabla \times \mathbf{v} = \mu \mathbf{v}$, μ being the corresponding eigenvalue. A detailed description can be found in [3]. Each eigenmode is characterized by a wave vector $\mathbf{k}$, so that $|\mu| = k$, and by the sign of μ, i.e., the helicity. An analytical expression for the helical eigenmode is

$$\mathbf{v}_{\mathbf{k}}^{\pm}(\mathbf{r}) = \frac{1}{\sqrt{2}}(\mathbf{b}_{\mathbf{k}} \pm i\hat{\mathbf{k}} \times \mathbf{b}_{\mathbf{k}}) e^{i\mathbf{k}\cdot\mathbf{r}} \equiv \mathbf{U}_{\mathbf{k}}^{\pm} e^{i\mathbf{k}\cdot\mathbf{r}}, \tag{1}$$

where $\hat{\mathbf{k}}$ is the unit vector parallel to $\mathbf{k}$, $\mathbf{b}_{\mathbf{k}}$ is an arbitrary unit vector orthogonal to $\mathbf{k}$ ($\mathbf{b}_{\mathbf{k}} \equiv \mathbf{b}_{-\mathbf{k}}$), and the sign $\pm$ stands for the eigenmode's helicity. The expansion of the 3D velocity field is

$$\mathbf{v}(\mathbf{r},t) = \sum_{\mathbf{k}} [a_{\mathbf{k}}^{+}(t)\mathbf{v}_{\mathbf{k}}^{+}(\mathbf{r}) + a_{\mathbf{k}}^{-}(t)\mathbf{v}_{\mathbf{k}}^{-}(\mathbf{r})], \tag{2}$$

where the summation is over the whole set of the wave vectors corresponding to a cubic box in the physical space with periodic boundary conditions.

The projection of the Euler equations onto the basis of the eigenstates (1) leads to the following set of equations for the complex amplitudes [3]:

$$\frac{d}{dt}a_{\mathbf{k}}^{\pm} = \frac{1}{2}\sum_{\mathbf{p}+\mathbf{q}=\mathbf{k}} [(p-q)(-M_{\mathbf{pq}-\mathbf{k}}^{\pm\pm\pm} a_{\mathbf{p}}^{\pm} a_{\mathbf{q}}^{\pm} + M_{\mathbf{pq}-\mathbf{k}}^{\mp\mp\pm} a_{\mathbf{p}}^{\mp} a_{\mathbf{q}}^{\mp}) + (p+q)(-M_{\mathbf{pq}-\mathbf{k}}^{\pm\mp\pm} a_{\mathbf{p}}^{\pm} a_{\mathbf{q}}^{\mp} + M_{\mathbf{pq}-\mathbf{k}}^{\mp\pm\pm} a_{\mathbf{p}}^{\mp} a_{\mathbf{q}}^{\pm})], \tag{3}$$

where the summation is carried out over all the wave vectors $\mathbf{p}$ and $\mathbf{q}$ whose sum is equal to a given wave vector $\mathbf{k}$. The coefficients of the triplet interactions are defined as

$$M_{\mathbf{pq}-\mathbf{k}}^{\mathcal{E}_1\mathcal{E}_2\mathcal{E}_3} \equiv \mathbf{U}_{\mathbf{p}}^{\mathcal{E}_1} \cdot (\mathbf{U}_{\mathbf{q}}^{\mathcal{E}_2} \times \mathbf{U}_{-\mathbf{k}}^{\mathcal{E}_3}), \tag{4}$$

where the vectors $\mathbf{U}$ are defined by Eq. (1) and the $\mathcal{E}$'s stand for the corresponding helicities.

We truncate the infinite set of equations (3), keeping only the amplitudes corresponding to the six wave vectors of an equal length k, which constitute the 3D simplex (tetrahedron) as shown in Fig. 1. Since each edge of the tetrahedron carries

two modes, one with positive and one with negative helicity, we thus condense Eqs. (3) into a DS for 12 complex variables. The chosen configuration provides an essential simplification, as, taking all the wave vectors with equal lengths, we nullify the terms proportional to $p-q$ in Eqs. (3).

In this work our objective is to single out and study in detail the simplest (*minimum*) nontrivial invariant subsystem that can be obtained as an invariant reduction of the full dynamical system for 12 complex variables. One can check that assuming three edges of the tetrahedron to carry only positive-H modes and three others to carry only negative-H ones, as shown in Fig. 1, is compatible with the full 12-dimensional system. Thus we obtain an invariant reduction to a system of equations for six variables. Calculation of the coefficients (4) demonstrates that nonzero coefficients of the reduced system take only two different values $\pm\sqrt{3}/2$. The eventual form of the six-dimensional system is

$$\frac{da_1}{dt}=a_4^*a_6, \tag{5}$$

$$\frac{da_2}{dt}=-a_1a_3^*, \tag{6}$$

$$\frac{da_3}{dt}=a_1a_2^*-a_5a_6^*, \tag{7}$$

$$\frac{da_4}{dt}=-a_1^*a_6+a_2a_5^*, \tag{8}$$

$$\frac{da_5}{dt}=-a_2a_4^*, \tag{9}$$

$$\frac{da_6}{dt}=a_3^*a_5, \tag{10}$$

where we have changed $t\to t/\sqrt{3}k$ and a_1–a_6 stand for the modes carried by the edges of the tetrahedron with the same numbers (Fig. 1).

Equations (5)–(10) (as well as the full 12-dimensional system) conserve three quantities. Two of them can be immediately identified as the energy and helicity of the flow

$$E=\sum_{n=1}^{6}|a_n|^2, \quad H=\sum_{n=1,4,5}|a_n|^2-\sum_{n=2,3,6}|a_n|^2. \tag{11}$$

The third integral is

$$I=\frac{1}{2}[(a_1a_5^*+a_1^*a_5)-(a_2a_6^*+a_2^*a_6)+(a_3a_4+a_3^*a_4^*)]. \tag{12}$$

Comparing the definitions (11) and (12), one can easily prove that $|H|\leqslant E$ and $|I|\leqslant\frac{1}{2}E$.

The only candidate for physical interpretation of this additional IM is the squared angular momentum. Indeed, the total momentum corresponding to the velocity field (2) is identically zero. The angular momentum of the same field is different from zero; however, it is obvious that the chosen way of truncation breaks the spatial isotropy and therefore breaks the angular momentum conservation too. Nevertheless, calculating the *squared* angular momentum corresponding to the truncated expansion (2) produces an expression (that we do not display here) that is similar to Eq. (12), although it contains some extra terms. We conjecture that the appearance of the additional IM is not an artifact of our model, but is naturally linked to the ''former'' conserved squared angular momentum.

Due to the obvious scale invariance of Eqs. (5)–(10), actual control parameters may be only the ratios H/E and I/E. Evidently, the available phase volume of the system is largest at $H=0$. In the opposite limit $H=E$ (or $H=-E$), the phase volume shrinks to zero. Indeed, in this limit Eqs. (11) tell us that $a_2=a_3=a_6=0$, while the remaining variables a_1, a_4, and a_5 take, according to Eqs. (5), (8), and (9), arbitrary constant values.

It is easy to consider analytically the limit case $(E-H)/E\to 0$. In this case one linearizes Eqs. (5), (8), and (9) with respect to the variables a_1, a_4, and a_5, which are expected to be small at small $(E-H)/E$, assuming the remaining amplitudes a_2, a_3, and a_6 constant. Looking for solutions to the system of the three linear equations in the form $a_1,a_4,a_5\sim e^{\gamma t}$, one can easily find three eigenvalues: $\gamma_1=0$ and $\gamma_{2,3}=\pm i\omega_0\equiv\pm i\sqrt{a_2^2+a_6^2}$. After adding small nonlinear terms, one may expect dynamical trajectories on the invariant spheres $a_1^2+a_4^2+a_5^2=\text{const}$ to be closed curves corresponding to periodic motions with frequencies close to ω_0. This suggests that the system (5)–(10) becomes nonchaotic in the limit $(E-H)/E\to 0$, which will be corroborated by the numerical results displayed below in Sec. III.

Further inspection of Eqs. (5)–(10) suggests splitting the full set of the variables into two subsets $A_1\equiv(a_1,a_4,a_5)$ and $A_2\equiv(a_2,a_3,a_6)$. The equations for each set can be represented in an explicitly Hamiltonian form. Indeed, the Hamiltonian (canonical) representation implies the existence of a Hamiltonian h and of a Poisson bracket (simplectic structure) [6] in the system's phase space. For any two functions $F(a_n)$ and $G(a_n)$ of the dynamical variables, the Poisson bracket is

$$\{F,G\}=\sum_{m,n}S_{mn}\frac{\partial F}{\partial a_m}\frac{\partial G}{\partial a_n}, \tag{13}$$

where the coefficient functions S_{mn} must be antisymmetric and they must satisfy the Jacobi identity [6]. Then the canonical equations of motion are written in terms of the Poisson bracket and the Hamiltonian as $da_n/dt=\{a_n,h\}$. As a consequence of this representation and the above-mentioned antisymmetry of S_{mn}, the Hamiltonian is conserved (unless it contains an explicit dependence upon time).

It is easy to check that the evolution equations for the sets A_1 and A_2 defined above can indeed be represented in the canonical form with the Hamiltonians

$$h_1=\sum_{n=1,4,5}a_na_n^*, \quad h_2=\sum_{n=2,3,6}a_na_n^*, \tag{14}$$

which are the combinations $\frac{1}{2}(E \pm H)$ of the conserved energy and helicity defined in Eqs. (11). The corresponding matrices of the coefficients $S_{m,n}$ in the Poisson brackets (13) are, respectively,

$$\begin{pmatrix} 0 & a_6 & 0 \\ -a_6 & 0 & a_2 \\ 0 & -a_2 & 0 \end{pmatrix} \tag{15}$$

for set A_1 and

$$\begin{pmatrix} 0 & -a_1 & 0 \\ a_1 & 0 & -a_5 \\ 0 & a_5 & 0 \end{pmatrix} \tag{16}$$

for A_2. Notice that the coefficient functions for each set depend upon the variables belonging to another set, i.e., one may regard these simplectic structures as time dependent. The Hamiltonians h_1 and h_2, which do not explicitly depend upon time, remain IM's even though the corresponding simplectic structures are time dependent.

To further simplify the dynamical system, we make use of the fact that Eqs. (5)–(10) are compatible with assuming that all the amplitudes a_n are real. What will be studied in detail in Sec. III is exactly this real reduction. Choosing h_1 and h_2 defined in Eqs. (14) as independent conserved quantities suggests to introduce, in the real case, the polar coordinates (θ_1, ϕ_1) and (θ_2, ϕ_2) in the two subspaces A_1 and A_2:

$$a_4 = \sqrt{h_1}\sin\theta_1, \quad a_1 = \sqrt{h_1}\cos\theta_1\cos\phi_1,$$

$$a_5 = \sqrt{h_1}\cos\theta_1\sin\phi_1,$$

$$a_3 = \sqrt{h_2}\sin\theta_2, \quad a_2 = \sqrt{h_2}\cos\theta_2\cos\phi_2,$$

$$a_6 = \sqrt{h_2}\cos\theta_2\sin\phi_2. \tag{17}$$

In terms of the polar coordinates, Eqs. (5)–(10) reduce to a four-dimensional dynamical system with the remaining conserved quantity I. In other words, the six-dimensional phase space of the real version of the system (5)–(10) is foliated into invariant four-dimensional subspaces corresponding to different values of E and H.

One may be tempted to conjecture that the six-dimensional DS with three conserved quantities must be integrable according to the Liouville theorem [6]. Nevertheless, direct simulations described below will clearly demonstrate that our DS easily generates chaotic trajectories, hence it cannot be integrable. The most plausible explanation for the lack of integrability is that the simplectic structure based on the two matrices (15) and (16) is very different from that for the standard Hamiltonian system with three degrees of freedom.

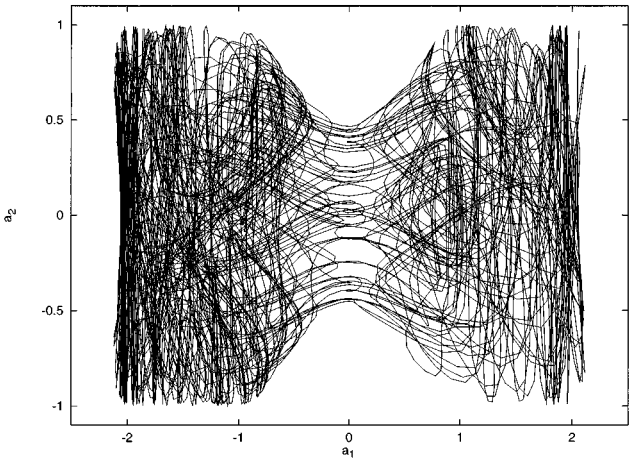

FIG. 2. Typical chaotic trajectory of the real dynamical system (6) at $H/E = 2/3$, $I/E = 1/3$ in the projection onto the plane (a_1, a_2). The system was integrated from $t = 0$ to $t = 1000$.

III. NUMERICAL RESULTS

As the source of the integration program, we employed the higher-order numerical code with the automatically adjusted step size [7]. For control of accuracy, conservation of all three IM's was continuously monitored. It was found that they preserved a constant value with the relative precision 10^{-6}. The reliability and accuracy of the numerical scheme were also checked by varying the fundamental time step.

A typical example of a chaotic dynamical trajectory at $H = 0$ is shown, in projection onto the plane (a_1, a_2), in Fig. 2. Since this trajectory seems to be chaotic, the next step is to compute a quantitative characteristic of chaos. The dynamical chaos implies that the trajectories are unstable in the linear approximation, i.e., an arbitrary infinitesimal perturbation $d(t)$ of a given trajectory grows in time exponentially, $d(t) \sim \exp[\int \lambda(t) dt]$, where $\lambda(t)$ is called the Lyapunov exponent. A standard characteristic of the chaos is $\lambda(t)$ averaged over a long trajectory, which will be denoted Λ. If the system is ergodic, then the result of averaging is the same for all the trajectories pertaining to the same set of values of the system's IM's (in the limit of infinitely long trajectories).

The general scheme of numerical computation of Λ can be found in Ref. [8]. We used the particular algorithm developed in [9]. Following this algorithm, one derives, first of all, the linearized version of the DS. Obviously, the eigenvalues λ of the linearized system, corresponding to an infinitesimal variation of a given trajectory, depend on the instantaneous values of the dynamical variables along the trajectory, i.e., they are functions of time. Next, one cuts a very long trajectory into short pieces. For each piece, one computes the eigenvalues and selects the largest one. Finally, Λ is obtained as an average of logarithms of all the instantaneous largest eigenvalues. The trajectory is really chaotic if thus computed Λ is positive.

Implementing this scheme of computation of Λ, we have checked that the mean value attains a nearly constant value and ceases to demonstrate any conspicuous variations after averaging over the time interval ~ 1000. Nevertheless, to confirm that the obtained values of Λ were indeed stabilized, some runs were extended up to the time 5000 and even 10 000.

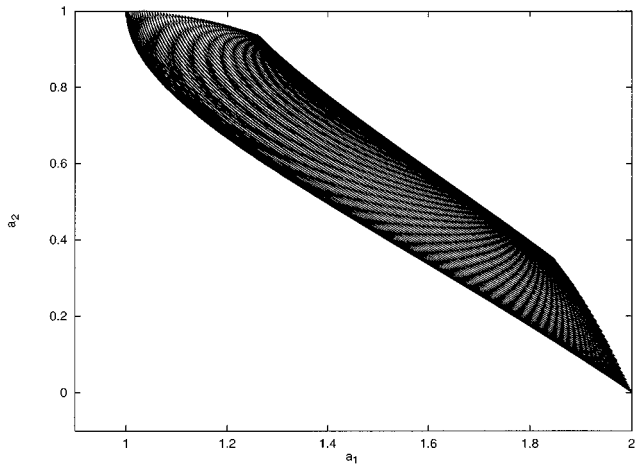

FIG. 3. Typical nonchaotic dynamical trajectory at $H/E=2/3$, $I/E=1/3$ in the projection onto the plane (a_1,a_2). The system was integrated from $t=0$ to $t=1000$.

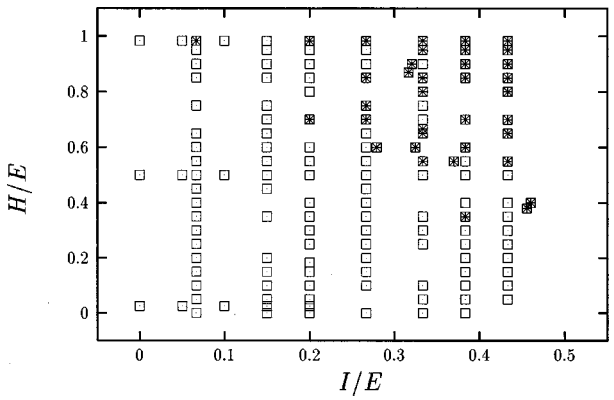

FIG. 4. Chart of the parametric plane $(H/E,I/E)$. The squares and ''Union Jacks'' are symbols for the spots where, respectively, the fully chaotic and mixed (chaotic or regular) behavior has been revealed by the simulations.

Scanning the phase space of our DS, we have found that at some values of the three IM's all the simulated trajectories are clearly chaotic, and in this case the corresponding averaged exponents Λ are indeed almost exactly equal (see below). At some other values of the IM's, we were able to find both chaotic and regular trajectories, depending on the particular choice of the initial point. In Fig. 3 we display a typical example of the regular trajectory found in this case and in Fig. 4 we show a (rather coarse) chart of the parametric plane $(H/E,I/E)$ in order to delineate a border between the ergodic (completely chaotic) region and the nonergodic one, where the mixed behavior has been found. The fact that a conservative DS may have ergodic and nonergodic regions in its phase space is well known [5].

In order to present the chaotic properties of the model in a more accurate form, in Fig. 5 we have plotted Λ vs H/E (using a logarithmic horizontal scale; see below) along six vertical cuts shown in Fig. 4 and in Fig. 6 Λ is plotted vs I/E along three horizontal cuts. As one sees from these plots, a noticeable feature of the plots is that $\Lambda(H/E)$ is monotonically decreasing, provided that the corresponding cuts do not cleave the nonergodic region of the mixed behavior. This seems quite natural because, according to Eq. (11), an increase of the helicity at a fixed value of the energy makes the available volume of the phase space smaller, hence the motion may be expected to be less chaotic. The dependence $\Lambda(H/E)$ demonstrates a nonmonotonic behavior (with some oscillations) if the corresponding cut is cleaving the nonergodic region.

Another noticeable feature is that, outside the regions of the mixed behavior, the points generated by different trajectories pertaining to the same set of values of the three IM's are fairly close to each other. This feature strongly suggests that the region in which all the trajectories are chaotic is indeed ergodic.

All the plots displayed in Fig. 5 show that, in accord with the simple analysis performed in Sec. II, the behavior of the system becomes nonchaotic in the limit $(E-H)/E\to 0$. However, an unexpected feature is that, quite typically, Λ keeps a nearly constant positive value up to $(E-H)/E$ very close to zero and then abruptly vanishes, demonstrating a very steep decrease. Because of this feature, we had to use the variable $\ln[E/(E-H)]$ as the abscissa in Fig. 5.

IV. THE COMPLEX DYNAMICAL SYSTEM

It is, of course, very important to check if the general properties of our *minimum* DS obtained by the deepest possible truncation of the Euler equations remain qualitatively the same in the framework of a truncation keeping more modes and thus, in a certain sense, standing closer to the underlying Euler equations. The first step in this direction is to consider the system (5)–(10) for six *complex* variables a_n. Recall that the complex system has the same three IM's E, H, and I as its real counterpart, while its actual phase space is 12 dimensional. Systematic simulations of the complex system is beyond the scope of this work; here, we only display, in Fig. 7(b), a typical example that allows one to compare the chaotic and regular dynamical trajectories in the real system and those in the complex one, obtained by adding a small imaginary part to the initial value of one of the dynamical variables a_n. In the case displayed in Fig. 7, the imaginary part was added to the initial value of a_1. It was taken to be $\sim\frac{1}{10}$ of the corresponding real part.

We observed that the small complex perturbation conspicuously alters the shape of the chaotic trajectory, which is in accord with the fact that all the chaotic trajectories are subject to a local instability. However, we have also observed that, most typically, the general character of the trajectory is not changed by the small initial complex perturbation: regular trajectories remain regular and chaotic ones remain chaotic.

Nevertheless, starting from a regular trajectory close to the border of the chaotic region, we could sometimes observe that the complex perturbation made the former regular trajectory chaotic. An example in shown in Fig. 7 [for the chaotic trajectory displayed in Fig. 7(b), $\Lambda=0.157$]. We have never observed the opposite effect, i.e., transformation of a chaotic trajectory into a regular one under the action of the complex perturbation.

Direct numerical evaluation of the LE demonstrates that a relatively small initial complex perturbation, although it does

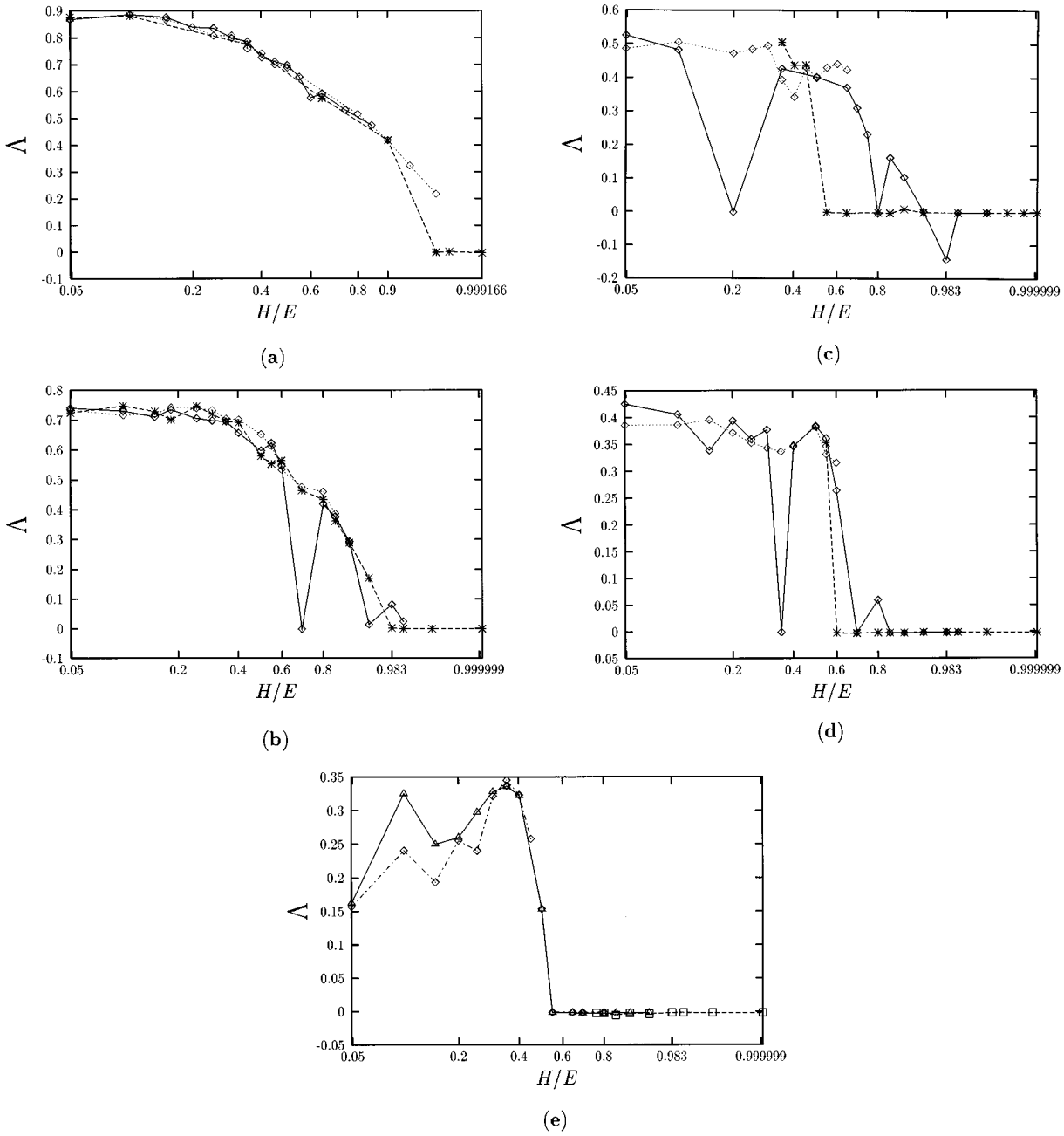

FIG. 5. Dependences of the mean Lyapunov exponent Λ upon H/E corresponding to six vertical cuts of the parameter plane of Fig. 4: (a) at $I/E=0.066$, (b) at $I/E=0.20$, (c) at $I/E=0.33$, (d) at $I/E=0.38$, and (e) at $I/E=0.43$. For the horizontal axis, we use $\ln[E/(E-H)]$ instead of E/H. The different symbols in these plots represent the values of Λ obtained for trajectories starting at initial points picked up, at given fixed values of all the three integrals of motion, by means of different auxiliary algorithms. In the case when the trajectory is nonchaotic, we set $\Lambda \equiv 0$.

not, generically, lead to a drastic qualitative change of the trajectory, results in a conspicuous change of its LE; for instance, in the case displayed in Fig. 7, the LE corresponding to the complex trajectory is 0.077, while the value of the LE for its real counterpart shown in Fig. 2 is 0.321. As a general trend, we have noticed that the LE for the complex trajectory is at least a factor of 2 *smaller* than for its real counterpart. This trend seems somewhat unexpected because the complex trajectory belongs to an essentially larger phase space than the real one and also because, as mentioned above, the complex perturbation could sometimes transform a regular trajectory into a chaotic one, but not vice versa. However, it is necessary to accumulate more numerical data in order to arrive at more definite conclusions concerning similarities and differences between the real and complex versions of our dynamical system.

V. THE DISSIPATIVELY PERTURBED MODEL

An issue of obvious interest is to add dissipative terms and a compensating gain to the conservative model considered above so as to lend it a chance to mimic turbulence of a viscous fluid. The simplest possibility is to replace Eqs. (5)–(10) by the equations

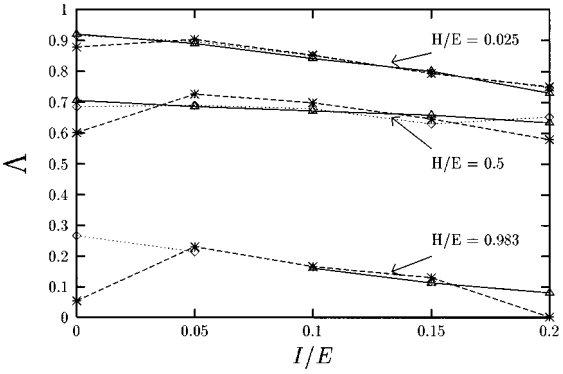

FIG. 6. Dependences of the mean Lyapunov exponent Λ upon I/E corresponding to three horizontal cuts of the parameter plane of Fig. 4. Different symbols have the same meaning as in Fig. 5.

$$\frac{da_1}{dt} = a_4^* a_6 + \gamma a_1 - \Gamma\left(\sum_{n=1}^{6} \left|a_n\right|^2\right) a_1, \tag{18}$$

$$\frac{da_2}{dt} = -a_1 a_3^* + \gamma a_2 - \Gamma\left(\sum_{n=1}^{6} \left|a_n\right|^2\right) a_2, \tag{19}$$

$$\frac{da_3}{dt} = a_1 a_2^* - a_5 a_6^* + \gamma a_3 - \Gamma\left(\sum_{n=1}^{6} \left|a_n\right|^2\right) a_3, \tag{20}$$

$$\frac{da_4}{dt} = -a_1^* a_6 + a_2 a_5^* + \gamma a_4 - \Gamma\left(\sum_{n=1}^{6} \left|a_n\right|^2\right) a_4, \tag{21}$$

$$\frac{da_5}{dt} = -a_2 a_4^* + \gamma a_5 - \Gamma\left(\sum_{n=1}^{6} \left|a_n\right|^2\right) a_5, \tag{22}$$

$$\frac{da_6}{dt} = a_3^* a_5 + \gamma a_6 - \Gamma\left(\sum_{n=1}^{6} \left|a_n\right|^2\right) a_6, \tag{23}$$

where $\Gamma > 0$ is an effective friction, $\gamma > 0$ is a compensating gain coefficient, and it is assumed that the friction and gain are added isotropically in the space of the variables a_n.

The IM's are no longer conserved in the presence of these perturbations. Instead, one can easily derive from Eqs. (18)–(23) the following evolution equation for the energy:

$$\frac{dE}{dt} = 2\gamma E - 2\Gamma E^2, \tag{24}$$

from which it follows that, in the limit $t \to \infty$, the energy takes the uniquely determined asymptotic value $E_0 = \gamma/\Gamma$. With regard to Eq. (24), the evolution of the former conserved quantities H and I is governed by the equations $dH/dE = H/E$ and $dI/dE = I/E$. From these equations it follows that, in the limit $t \to \infty$, H and I take the limit values $H_0 = (H_{\rm in}/E_{\rm in})E_0$ and $I_0 = (I_{\rm in}/E_{\rm in})E_0$, where $H_{\rm in}$, $I_{\rm in}$, and $E_{\rm in}$ are initial values of the former IM's. Finally, it follows from Eqs. (18)–(23) that, asymptotically, the motion governed by these equations will be the same as that governed by the conservative equations (5)–(10) in the particular case when E, H, and I take the values E_0, H_0, and I_0. Thus this simplest dissipative generalization asymptotically amounts to a particular case of the conservative system.

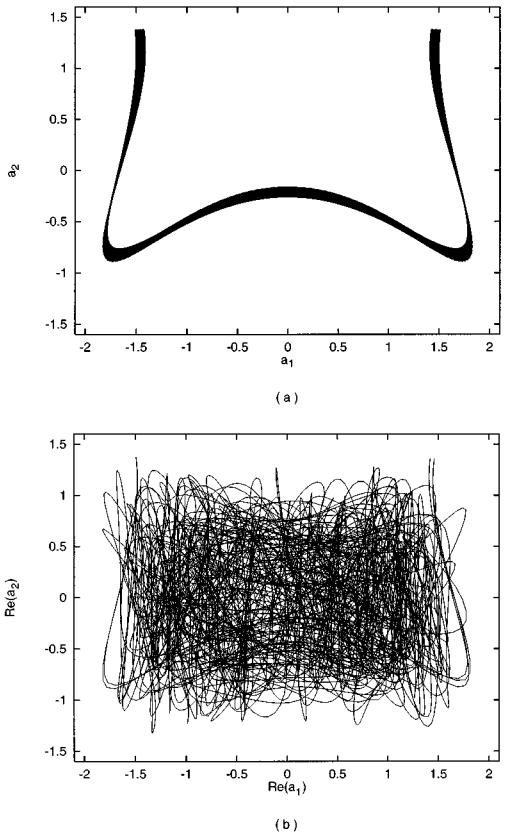

FIG. 7. Example of transformation of a regular real trajectory (a) into a chaotic one and (b) under the action of a small complex perturbation of the initial point.

VI. CONCLUSION

In this work we have derived a Hamiltonian dynamical system, projecting the 3D Euler equations onto a basis composed of six wave vectors closed into a regular tetrahedron. We have derived a system of six equations for complex amplitudes of the flow, with three integrals of motion. The system admits reduction to six real equations for three positive-helicity and three negative-helicity modes, which is the minimum truncation of the 3D Euler equations. We have simulated the latter system numerically and have demonstrated that it is chaotic despite having three itegrals of motion in its six-dimensional phase space. The simulations reveal that the dynamics is fully chaotic in a part of the system's phase space, while in another part it mixes chaotic and regular trajectories. We computed the mean Lyapunov exponent Λ characterizing the local instability of the trajectories. We have found that Λ is nearly independent of the choice of the trajectory in the chaotic region, i.e., this region appears to be ergodic.

An issue of profound importance is to understand if the behavior of the dynamical system can really mimic the 3D Euler equations, from which the dynamical system was ob-

tained by truncation. To check this, the next relevant step is to consider a system generated by projection of the Euler equations onto a larger basis. In practical terms, this implies, first of all, to simulate the full system of the complex equations (5)–(10). In this work we did not display systematic results for the complex system. Nevertheless, on the basis of more limited simulations, we have concluded that a small complex perturbation does not generically lead to a qualitative change of the system's dynamics, although a change in the Lyapunov exponent may be quite conspicuous. A simple dissipative modification of the model was considered too and it was demonstrated that this generalization actually amounts to a special case of the conservative model.

ACKNOWLEDGMENTS

We are indebted to L. A. Bunimovich, P. Grassberger, and A. S. Pikovsky for useful discussions. R.M. appreciates the hospitality of the Faculty of Engineering at the Tel Aviv University. B.A.M. and R.M. gratefully acknowledge support from Ormat Industries Ltd. (Yavneh, Israel). R. M. extends her gratitude to B. Bacchi for his encouraging support.

[1] L. Sirovich, Physica D **37**, 126 (1989).
[2] L. Sirovich and X. Zhou, Phys. Rev. Lett. **72**, 340 (1994).
[3] G. Knorr, J. P. Lynov, and H. L. Pécseli, Z. Naturforsch. Teil A **45**, 1059 (1990).
[4] J. C. André and M. Lesieur, J. Fluid Mech. **81**, 187 (1977).
[5] A. J. Lichtenberg and M. A. Lieberman, *Regular and Chaotic Dynamics* (Springer-Verlag, New York, 1992).
[6] V. I. Arnold, *Mathematical Methods of Classical Mechanics* (Nauka, Moscow, 1974).
[7] This code is available at un2sun1.unige.ch:pub/doc.math.
[8] T. S. Parker and L. O. Chua, *Practical Numerical Algorithms for Chaotic Systems* (Springer-Verlag, Berlin, 1989).
[9] H. Bai-lin, in *Directions in Chaos*, edited by H. Bai-Lin (World Scientific, Singapore, 1988), Vol. 2, p. 294.